



VOLUME 47

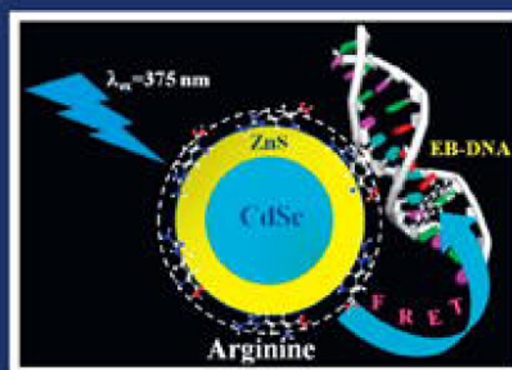
ISSUE 8

AUGUST 2012

MATERIALS RESEARCH BULLETIN

AN INTERNATIONAL JOURNAL REPORTING RESEARCH ON
THE SYNTHESIS, STRUCTURE, AND PROPERTIES OF MATERIALS

Preparation of water soluble L-arginine capped cdSe/ZnS QDs and
their interaction with synthetic DNA: Picosecond-resolved FRET study



A. Giri, N. Goswami, P. Lemmens, S.K. Pal



Contents lists available at SciVerse ScienceDirect

Materials Research Bulletin

journal homepage: www.elsevier.com/locate/matresbu

Preparation of water soluble L-arginine capped CdSe/ZnS QDs and their interaction with synthetic DNA: Picosecond-resolved FRET study

Anupam Giri^a, Nirmal Goswami^a, Peter Lemmens^b, Samir Kumar Pal^{a,*}

^a Department of Chemical, Biological & Macromolecular Sciences, S. N. Bose National Centre for Basic Sciences, Block JD, Sector III, Salt Lake, Kolkata 700 098, India

^b Institute for Condensed Matter Physics, Technical University of Braunschweig, Mendelssohnstr. 3, 38106 Braunschweig, Germany

ARTICLE INFO

Article history:

Received 17 December 2011
Received in revised form 28 February 2012
Accepted 17 April 2012
Available online 24 April 2012

Keywords:

A. Semiconductors
A. Organic compounds
A. Polymers
C. Electron microscopy
D. Surface properties

ABSTRACT

We have exchanged TOPO (trioctylphosphine oxide) ligand of CdSe/ZnS core/shell quantum dots (QDs) with an amino acid L-arginine (Arg) at the toluene/water interface and eventually rendered the QDs from toluene to aqueous phase. We have studied the interaction of the water soluble Arg-capped QDs (energy donor) with ethidium (EB) labeled synthetic dodecamer DNA (energy acceptor) using picoseconds resolved Förster resonance energy transfer (FRET) technique. Furthermore, we have applied a model developed by M. Tachiya to understand the kinetics of energy transfer and the distribution of acceptor (EB-DNA) molecules around the donor QDs. Circular dichroism (CD) studies revealed a negligible perturbation in the native B-form structure of the DNA upon interaction with Arg-capped QDs. The melting and the rehybridization pathways of the DNA attached to the QDs have been monitored by the CD which reveals hydrogen bonding is the associative mechanism for interaction between Arg-capped QDs and DNA.

© 2012 Elsevier Ltd. All rights reserved.

1. Introduction

Semiconductor quantum dots (QDs) have attracted great interest over the past decade due to their unique optical properties, such as a bright, narrow and tunable fluorescence signatures, broad excitation but specific emission spectra and good photochemical stability [1–3]. Because of these distinct optical properties, QDs are being extensively explored with respect to biomedical use as imaging contrast agents, traceable therapeutic vectors and for energy applications including photovoltaic solar cells [4–7]. However, their advantageous properties are undermined by the inherent insolubility of QDs in aqueous solution. While, water solubilization of QDs is essential for many biological applications, it presents a significant challenge. Use of mercaptoacetic acid ligands was one of the first strategies applied to produce water soluble QDs [8]. Since then, a number of other thioalkyl acid ligands have been used, including 3-mercapto-propionic acid [9,10] and dihydrolipoic acid [11]. These ligands form a self-assembly on the surface of the QDs that proceeds via a metal-thiol affinity interaction and other polar groups of the ligands are exposed to the surrounding aqueous solution [12]. Other approaches using non-thiol based organic ligands have also been employed including 4-substituted pyridine, oligomeric phosphine, poly (dimethylaminoethyl)

methacrylate [13], polymers [14], amphiphilic polymers [15,16] and phospholipids [17]. There has been a growing emphasis on assembling biological molecules to the water-soluble QDs through different types of interactions. In most cases these interactions involve covalent conjugation or simple adsorption of the biological molecules to the solubilizing layer around the QDs [8,9,14,18]. In addition to these, the formations of nanobioconjugates through various nonspecific interactions (electrostatic, hydrogen-bonding interactions, etc.) between biological molecules and nanoparticles have also been explored [1,19–21].

To date, CdSe/ZnS core/shell QDs remain among the best available for many biological applications [6,22,23]. However, QDs synthesized in organic solvents contain hydrophobic surface ligands such as trioctylphosphine oxide (TOPO), trioctylphosphine (TOP) [24], tetradecylphosphonic acid (TDPA) or oleic acid [25]. As a result they are insoluble in water and in other protic solvents namely methanol or ethanol [26]. So, their biological applications are restricted, where water solubility is highly desirable. Hence, the main challenge, to make quantum dots soluble in water for their further prospective bioconjugate reactions, remains.

Amino acids are inherently biocompatible and among common amino acids L-arginine along with Lysine are positively charged. Upon functionalization of nanoparticle with these amino acids, the nanoparticles become positively charged and their interaction with the negatively charged biomolecules is much more efficient. However, in comparison with Lysine, due

* Corresponding author. Tel.: +91 3323355708; fax: +91 3323353477.
E-mail address: skpal@bose.res.in (S.K. Pal).

to the presence of a guanidyl group, arginine molecules can highly facilitate the interaction of nanoparticle with biological macromolecules [27].

In the present work, we have exploited the toluene/water interface to replace the original TOPO capping of CdSe/ZnS core/shell QDs dispersed in toluene, with a natural amino acid L-arginine (Arg) using the reactivity of the amine groups. This allows a dispersal of the QDs in aqueous solutions with a quantum yield of 14%. We have confirmed the conjugation of arginine molecules with the QDs by using FTIR spectroscopy. The structural integrity of the QDs upon water solubilization has been confirmed with HRTEM. Using picosecond-resolved photoluminescence measurements, we have explored an efficient ultrafast energy transfer from Arg-capped CdSe/ZnS QDs (donor) to Ethidium bromide-labeled-DNA (acceptor) applying the sensitivity of FRET. Employing the kinetic model developed by Tachiya (for the quenching of luminescent probes), we have also analyzed the picosecond-resolved photoluminescence measurement results to understand the kinetics of energy transfer with the dye labeled DNA and the distribution of acceptor (EB-DNA) molecules around the donor QDs, as it is a driving factor for efficient energy transfer and for the accurate donor-acceptor measurements. In order to confirm any structural perturbation of dodecamer DNA in the nanobioconjugate, circular dichroism (CD) studies have also been performed on both the DNA and DNA-QD conjugate. To investigate in more details the type of interaction taking place between the QDs and DNA, using CD we have monitored the melting and rehybridization pathways of the dodecamer DNA, conjugated to the QDs. This reveals that hydrogen bonding is the accompanied mechanism involved during the formation of this QD-DNA nanobioconjugate.

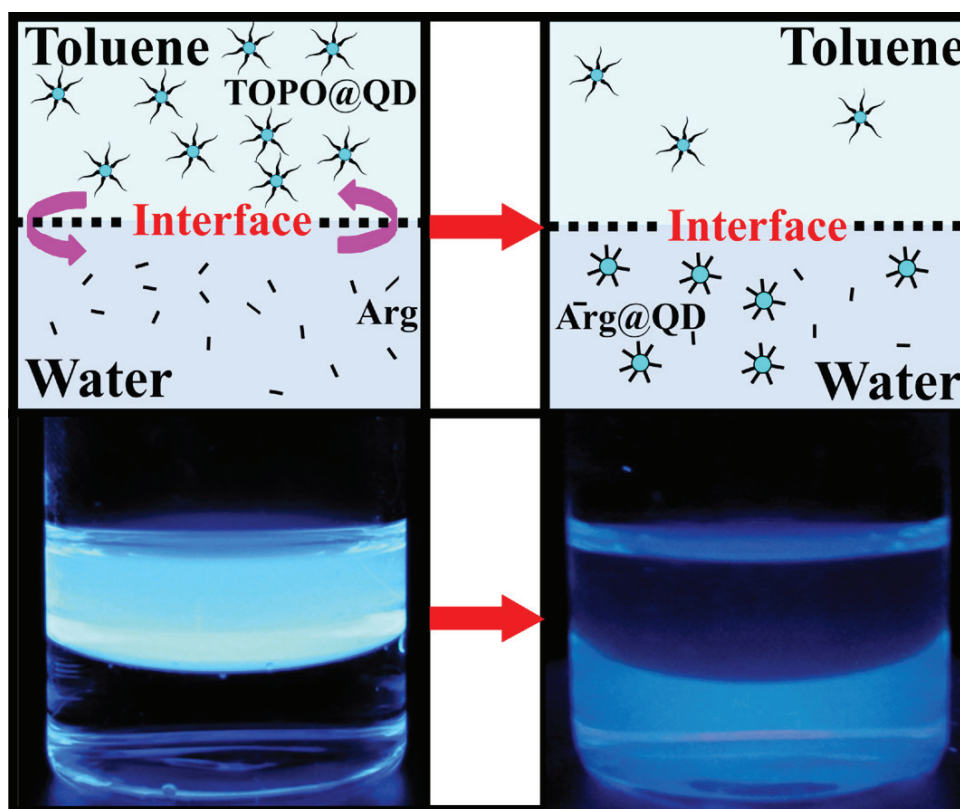
2. Experimental

2.1. Materials and instrumentations

Lake Placid Blue CdSe/ZnS core/shell semiconductor nanocrystals (QDs) in toluene were purchased from Evident Technologies (Troy, NY) and had an emission maximum at 483 nm. L-Arginine hydrochloride (minimum 98%) was purchased from Sigma (USA) and was used as received without further purification. Phosphate buffer was obtained from Sigma. The dye Ethidium bromide (EB) was obtained from Molecular Probes. Steady-state absorption and emission were measured with a Shimadzu UV-2450 spectrophotometer and Jobin Yvon Fluoromax-3 fluorimeter respectively. A JASCO FT/IR-6300 spectrometer was used for the Fourier transform infrared spectroscopy (FTIR), to confirm the interaction of arginine molecules with the QDs. For FTIR measurements, powdered arginine capped QDs sample was mixed with KBr powder and pelletized. The background correction was made by using a reference blank of a KBr pellet. Circular dichroism (CD) experiments were done in a JASCO 815 spectropolarimeter. TEM samples were prepared by dropping sample stock solution onto a 300-mesh carbon coated copper grid and dried overnight in air under an electric lamp. Particle sizes were determined from micrographs recorded at a magnification of 450,000 \times using a FEI Tecnai TF-20 field-emission high-resolution transmission electron microscope operating at 200 kV.

2.2. Preparation of water-soluble arginine capped QDs

The TOPO-capped CdSe/ZnS core/shell QDs in toluene were rendered water-soluble by ligand exchange with L-arginine,



Scheme 1. Trioctylphosphine oxide (TOPO) stabilized CdSe/ZnS quantum dots (QD) were modified with L-arginine via ligand exchange. Phase transfer of arginine-modified QDs from toluene phase into water was achieved by using the reactivity of amine group of arginine. Upon replacement of the initial TOPO ligand with arginine the emission of the QDs is decreased.

following a simple process (Scheme 1) using the reactivity of the amine group (of L-arginine) with the ZnS shell of the QDs. The addition of 5 ml of the QDs toluene suspension into about 5 ml of the L-arginine aqueous solution (pH ~ 9) under vigorous stirring results in the formation of toluene-in-water microdroplets. The sample was stirred overnight, settled for 3 h and then the aqueous phase was separated and analyzed by UV-vis, fluorescence spectroscopy and HRTEM. We have calculated the quantum yield of arginine capped QDs following an equation [28], which relates the natural lifetime (τ_n), quantum yield (Q) and measured lifetime (τ) of a fluorescence species by,

$$\tau_n = \frac{\tau}{Q}$$

Since the natural radiative lifetime of a fluorescence species is the sole property of the material and it is only the measured lifetime which varies depending upon the local environment of the fluorescence species. So, we have exploited the measured lifetime ($\tau = 7.70$ ns) along with the quantum yield (40%) of TOPO capped CdSe/ZnS QDs in toluene as reference and using the measured lifetime of arginine capped QDs in water ($\tau = 2.70$ ns), we have calculated the quantum yield of arginine capped QDs.

2.3. Preparation of DNA samples

The DNA oligomer having sequence CTTTTCAAAAG was obtained from Sigma-Aldrich and used as received. All aqueous solutions were prepared in 50 mM phosphate buffer of pH 7 using water from the Millipore system. To reassociate the single strand DNA into self-complementary double-strand DNA (CTTTTC-AAAAG)₂, thermal annealing was performed as per the methodology prescribed by the vendor. The nucleotide concentration was determined by absorption spectroscopy using the average extinction coefficient per nucleotide of the DNA (6600 M⁻¹ cm⁻¹ at 260 nm). The EB-DNA complex solution was prepared by adding the requisite amount of probe stock solution to DNA followed by 1 h of magnetic stirring. To ensure complete complexation of EB with the DNA, the probe concentration was made much less (8 μM) than that of the DNA (30 μM) ([EB-DNA] = 8 μM) for the FRET studies.

2.4. Time resolved spectroscopy

Picosecond-resolved fluorescence decay transients were measured by using a laser source of 375 nm wavelength and a commercially available spectrophotometer (Life Spec-ps, Edinburgh Instruments, UK) with 60 ps instrument response function (IRF). The observed fluorescence transients were fitted by using a nonlinear least square fitting procedure to a function ($X(t) = \int_0^t E(t')R(t-t')dt'$) comprising of a convolution of the IRF ($E(t)$) with a sum of exponentials ($R(t) = A + \sum_{i=1}^N B_i e^{-t/\tau_i}$) with pre-exponential factors (B_i), characteristic lifetimes (τ_i) and a back ground (A). The relative concentration in a multi exponential decay was finally expressed as:

$$c_n = \frac{B_n}{\sum_{i=1}^N B_i} \times 100$$

The quality of the curve fitting was evaluated by reduced chi-square and residual data.

To estimate the FRET efficiency of the donor and hence to determine the distance of the donor-acceptor pair, we followed the methodology described in Chapter 13 of Ref. [28]. The Förster distance (R_0) is given by,

$$R_0 = 0.211[\kappa^2 n^{-4} Q_D J(\lambda)]^{1/6} \quad (\text{in } \text{Å}), \quad (1)$$

where κ^2 is a factor describing the relative orientation in space of the transition dipoles of the donor and acceptor. We assumed that

the orientation factor κ^2 is equal to the dynamic average of 2/3 which is not a major deviation from real fact of randomized donor and acceptor orientations in an ensemble. Moreover, a variation of κ^2 does not seem to have resulted in major errors in the calculated distances. The refractive index (n) of the medium was assumed to be 1.4. $J(\lambda)$, the overlap integral, which expresses the degree of spectral overlap between the donor emission and the acceptor absorption, is given by,

$$J(\lambda) = \frac{\int_0^\infty F_D(\lambda)\epsilon(\lambda)\lambda^4 d\lambda}{\int_0^\infty F_D(\lambda)d\lambda} \quad (2)$$

where $F_D(\lambda)$ is the fluorescence intensity of the donor in the wavelength range of λ to $\lambda + d\lambda$ and is dimensionless. $\epsilon(\lambda)$ is the extinction coefficient (in M⁻¹ cm⁻¹) of the acceptor at λ . If λ is in nm, then J is in units of M⁻¹ cm⁻¹ nm⁴.

Once the value of R_0 is known, the donor-acceptor distance (R) can easily be calculated using the formula,

$$R^6 = \frac{R_0^6(1-E)}{E}, \quad (3)$$

here E is FRET efficiency, measured by using the lifetimes of the donor in the absence (τ_D) and presence (τ_{DA}) of acceptor which is defined as,

$$E = \frac{1 - \tau_{DA}}{\tau_D} \quad (4)$$

It has to be noted that Eq. (4) holds rigorously only for a homogeneous system (i.e. identical donor-acceptor complexes) in which the donor and the donor-acceptor complex have single exponential decays. However, for donor-acceptor systems decaying with multi-exponential lifetimes, FRET efficiency (E) is calculated from the amplitude weighted lifetimes ($\langle \tau \rangle = \sum_i \alpha_i \tau_i$ where α_i is the relative amplitude contribution to the lifetime τ_i). We have used the amplitude weighted time constants for τ_D and τ_{DA} to evaluate E using Eq. (4).

3. Results and discussion

3.1. Ligand exchange

As Scheme 1 illustrates, the addition of QDs toluene suspension into the aqueous solution of L-arginine (pH ~ 9) under vigorous stirring condition results in the formation of toluene microdroplets, and the QDs in toluene get the chance to interact strongly with the arginine molecules through the liquid-liquid interface [29,30]. Photo images of the QDs under UV excitation before and after ligand exchange clearly indicate the successful phase transfer of the QDs from toluene into the aqueous medium. Efficient ligand exchange through this process is driven by an interaction between the amine group of the stabilizing amino acid in the aqueous phase and the ZnS shell of the QDs in the toluene phase at the interface [31,32]. Computational studies have shown that primary amines have greater surface binding energy than carboxylic acids, though lower binding energy compared to TOPO and phosphonic acids [33–35]. However, primary amines have the advantage of more complete surface coverage which can theoretically reach 100% – over TOPO (30% coverage) due to reduced steric effects [36].

3.2. Characterization of arginine capped QDs

To obtain direct evidence for the arginine functionalization of QDs, FTIR measurements were performed on both the free arginine molecules and arginine molecules attached to the QDs. The FTIR spectra of arginine capped QDs and free arginine molecules are shown in Fig. 1. For arginine, the characteristic band at 3161 cm⁻¹

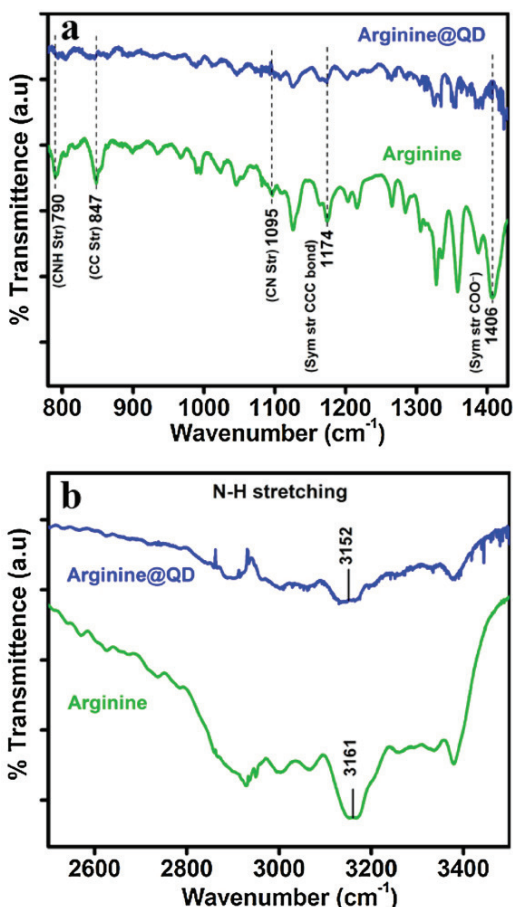


Fig. 1. FTIR spectra of free arginine molecules and arginine molecules attached to the QDs: (a) spectral broadening of C–N–H, C–C and C–C–C stretching frequencies of arginine upon interaction with the QDs. Perturbation of C–N and COO⁻ stretching frequencies of arginine is also observed after interaction with the QDs. (b) Spectral broadening and red shift of N–H stretching frequency of arginine upon interaction with the QDs.

(Fig. 1b) corresponding to the N–H stretching mode [37], is broadened and red-shifted to 3152 cm⁻¹, suggesting its interaction with the QD surface. Moreover, as shown in Fig. 1a, the significant perturbation of other characteristic bands of arginine at 790 cm⁻¹ (C–N–H stretching), 847 cm⁻¹ (C–C stretching), 1095 cm⁻¹ (C–N stretching), 1174 cm⁻¹ (C–C–C symmetric stretching) and 1406 cm⁻¹ (COO⁻ symmetric stretching) [37,38] also confirms the binding of arginine molecules to the QD surface.

The direct interaction of arginine molecules with the QDs surfaces ensured that the overall size of the QDs remains unchanged, with a thin solubilizing shell. Inset of Fig. 2a shows the HRTEM images of Arg-capped QDs in water, which reveal the diameters of the QDs to be 3.2 nm. The existence of lattice fringes illustrates the highly crystalline nature of the QDs.

3.3. Interaction of arginine capped QDs with DNA: FRET study

We have employed FRET to study the interaction of the synthetic dodecamer DNA (EB labeled) with the water soluble QDs (pH ~ 7). Fig. 2a shows the spectral overlap between the emission spectrum of arginine capped QDs (donor) and the absorption spectrum of EB-labeled DNA (acceptor), suggesting the possibility of efficient Förster resonance energy transfer (FRET) between the donor and the acceptor, when EB-labeled DNA becomes adsorbed at the surface of the arginine capped QDs. Fig. 2b represents the

steady state photo luminescence (PL) quenching of the donor (arginine capped QDs) in presence of EB-labeled DNA. Picosecond resolved PL transients (Fig. 2c) of both donor and donor–acceptor systems monitored at 485 nm, shows significant shortening in the QDs fluorescence lifetime upon adsorption of EB-labeled DNA at the QDs surface. The picosecond resolved fluorescence decay of arginine capped QDs (donor) in buffer revealed multiexponential time constants of 0.08 ns (45%), 1.15 ns (25%) and 8.50 ns (29%) giving an average time constant ($\langle\tau\rangle$) of 2.80 ns. For the donor–acceptor system (arginine capped QDs–EB labeled DNA) time constants are obtained as 0.09 ns (72%), 1.23 ns (18%) and 5.40 ns (8%) giving an average time constant ($\langle\tau\rangle$) of 0.72 ns (Table 1). The substantial shortening in the QDs excited state lifetime upon conjugate formation indicates conclusively that efficient FRET occurs from the QD donor to the EB-DNA acceptor. Taking the calculated quantum yield of Arg-capped QDs in absence of acceptor as 0.14 and based on the spectral overlap, we have estimated a FRET efficiency of 74% using Eq. (4). The measured Förster distance, R_0 , for the QD–DNA nanobioconjugate is 2.88 nm. The donor–acceptor distance (R) calculated using Eq. (3) is 2.42 nm (Table 1).

3.4. Interaction of arginine capped QDs with DNA: kinetic model of Tachiya

For better understanding of the energy transfer between the excited state of QDs with EB-DNA, it is essential to know the distribution of acceptor molecules around the QDs because this is a governing factor that can influence the efficient energy transfer as observed from the time resolved fluorescence studies. In this regard, we have applied a kinetic model developed by Tachiya for the quenching of luminescent probes [39,40]. The excited state decay of the QDs may be described by the following kinetic model assuming a competition of the energy transfer with unimolecular decay processes:

$$P_n^* \xrightarrow{k_0} P_n \quad (5)$$

$$P_n^* \xrightarrow{k_q} P_n \quad (6)$$

where P_n^* stands for excited state QDs with n number of EB-DNA molecules attached, while P_n stands for ground state QDs with n number of EB-DNA molecules attached. k_0 is the total decay constant of the QDs in excited state in absence of the acceptor molecule. k_q is the rate constant for energy transfer for one EB-DNA molecule. In this model, it is assumed that the distribution of the number of acceptor molecules (EB-DNA) attached to one QDs follows a Poisson distribution [40], namely:

$$p(n) = \left(\frac{m^n}{n!}\right) \exp(-m), \quad (7)$$

where m is the mean number of EB-DNA molecules attached to one QD and

$$m = \frac{k_+ [A]}{k_-}, \quad (8)$$

where k_+ is the rate constant for attachment of a EB-DNA molecule to a QD, while k_- is the rate constant for detachment of a EB-DNA molecule from the QD. $[A]$ stands for the concentration of EB-DNA molecule in the aqueous phase. Based upon the above model, the equation for the total concentration $P^*(t)$ of excited state QDs at time t is given by [40]:

$$P^*(t) = P^*(0) \exp \left[- \left(k_0 + \frac{k_0 k_+ [A]}{k_- + k_q} \right) t - \frac{k_q^2 k_+ [A]}{k_- (k_- + k_q)^2} \times \{1 - \exp[-(k_- + k_q)t]\} \right]. \quad (9)$$

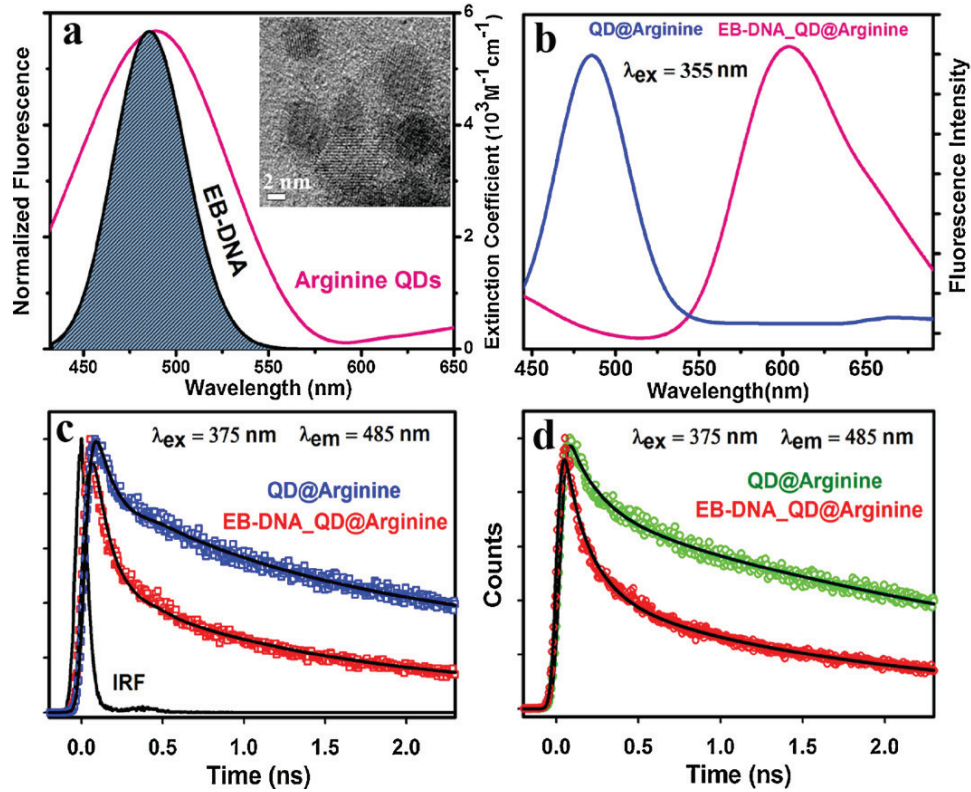


Fig. 2. (a) Spectral overlap between emission spectrum of arginine-capped CdSe/ZnS core/shell QDs and the absorption spectrum of EB-labeled DNA (the extinction coefficient value is for the acceptor, EB-labeled DNA). Inset shows the HRTEM image of QD in toluene. (b) Steady-state fluorescence quenching of arginine-capped QDs in presence of the acceptor EB-DNA (c) Picosecond-resolved PL transients of arginine-capped CdSe/ZnS QDs and (EB-DNA)-QD complex monitored at $\lambda_{em} = 485$ nm. (d) Picosecond-resolved PL transients of arginine-capped CdSe/ZnS QDs and (EB-DNA)-QD complex, fitted with Tachiya kinetic model. The fitted curves are shown in black.

If k_- is much smaller than k_q , Eq. (9) reduces to:

$$P^*(t) = P^*(0)\exp\{-k_0t - m[1 - \exp(-k_qt)]\}. \quad (10)$$

In our system, along with the acceptor EB-DNA molecules, there exist some unidentified traps on the surface of the QDs and these are also taken into account. If the distribution of the number of unidentified traps on the surface of the QDs follows a Poisson distribution with the average number (m_t), the decay curves of the excited state of QDs in the absence and presence of dye molecules are described by [41]:

$$P^*(t, 0) = P^*(0)\exp\{-k_0t - m_t[1 - \exp(-k_{qt})]\} \quad (11)$$

and

$$P^*(t, m) = P^*(0)\exp\{-k_0t - m_t[1 - \exp(-k_{qt})] - m[1 - \exp(-k_qt)]\}, \quad (12)$$

where the quenching rate constant (k_{qt}) by unidentified traps may be different from that (k_q) by acceptor EB-DNA molecules. We have determined the values of the parameters m_t , k_{qt} , k_0 , m , and k_q by

fitting Eqs. (11) and (12) to the decay curves in the absence and presence of acceptor EB-DNA molecules.

Fig. 2d shows the time resolved fluorescence transients of CdSe/ZnS QDs in absence and presence of EB-DNA molecules and black curves represents the result of fitting the curves with Eqs. (11) and (12). The observed fluorescence transients were fitted using a nonlinear least squares fitting procedure (software SCIENTIST™) to a function ($X(t) = \int_0^t E(t')P(t-t')dt'$) comprising of the convolution of the instrument response function (IRF) ($E(t)$) with exponential ($P(t, m) = P(0)\exp\{-k_0t - m_t[1 - \exp(-k_{qt})] - m[1 - \exp(-k_qt)]\}$). The purpose of this fitting is to obtain the decays in an analytic form suitable for further data analysis. As evident from Fig. 2d, the fitting of the decay curves according to the model is reasonably well. The quenching parameters are summarized in Table 2. The quenching rate constant (k_{qt}) due to unidentified traps on the surface of the nanocrystals are the same even after addition of acceptor (EB-DNA) molecules, and this indicates the average number of unidentified trap states to be the same. However, it is observed from Table 2 that the average number of unidentified traps state increases with addition of acceptor molecules. Since, there are still many unknown parameters in the QDs excitation dynamics, for an accurate

Table 1

Fitted decay time constants of QD and QD-(EB-DNA) complex from picosecond experiments. Values in parentheses represent the relative weight percentage of the time components.

System	τ_1 [ps]	τ_2 [ps]	τ_3 [ps]	$\langle \tau \rangle$ [ps]
QD	85 (45)	1153 (26)	8527 (29)	2799
QD-EB-DNA	98 (73)	1239 (19)	5403 (8)	726

Table 2

Overview of the value of quenching parameters using a kinetic model.

System	k_0 [ns ⁻¹]	m_t	k_{qt} [ns ⁻¹]	m	k_q [ns ⁻¹]
QD	0.28	0.40	4.60	-	-
QD-EB-DNA	0.28	1.06	4.67	1.15	0.20

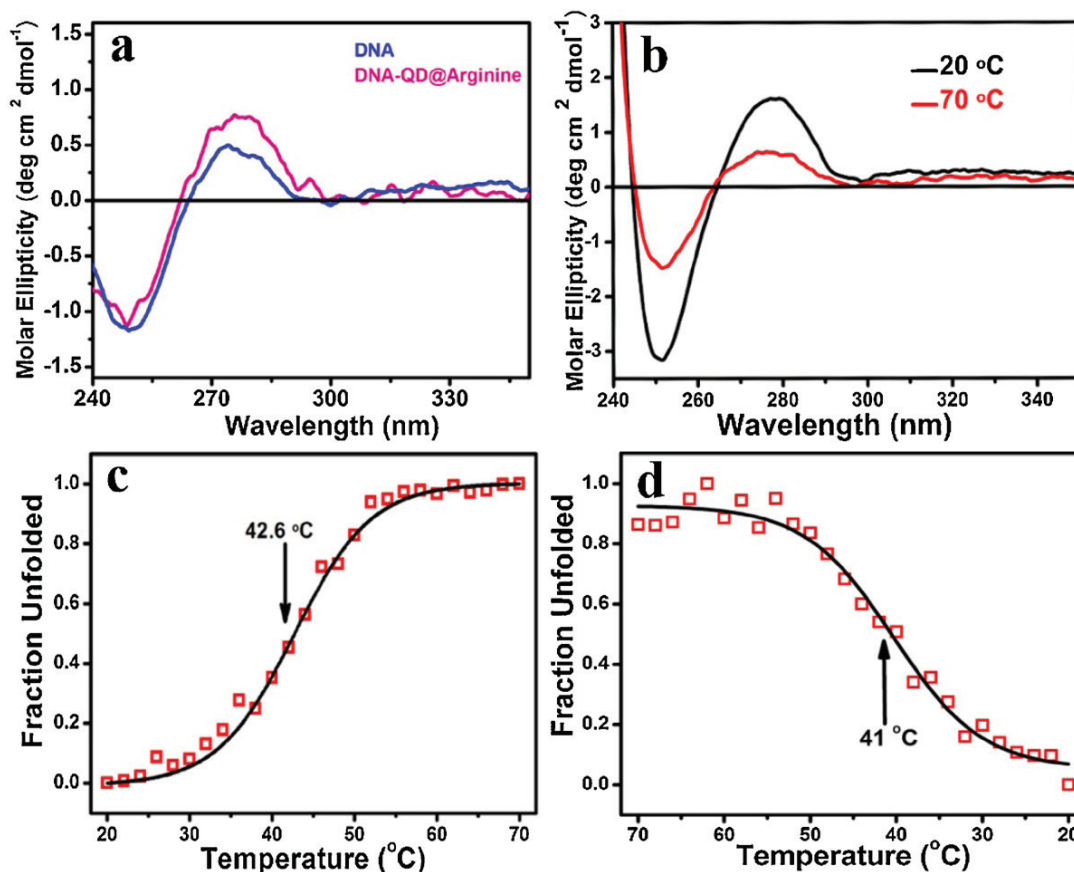


Fig. 3. (a) Circular dichroism (CD) spectra of dodecamer DNA and dodecamer DNA conjugated to QDs. Structural integrity of the DNA in the QD–DNA conjugate is clearly evident. (b) CD spectra of dodecamer DNA–QD conjugates at two different temperatures. (c) and (d) The melting and rehybridization of dodecamer DNA conjugated to QDs. Solid lines are the fitted sigmoidal curve.

interpretation of this observation a more complex model and a larger data set is required. As summarized in Table 2, the mean number of acceptor (EB-DNA) molecules associated with the QDs is 1.15 and the estimated rate constant for energy transfer (k_q) per acceptor molecules is 0.20 ns^{-1} . The energy transfer rate calculated from conventional FRET model is found to be somewhat different (1.01 ns^{-1}) from the value obtained using Tachiya's model (0.20 ns^{-1}). However, as shown in Table 1, the contribution of the longer lifetime (8.52 ns) in the overall average lifetime of the donor is significant. Other lifetime values of 1.15 ns and 0.08 ns could be associated with the unidentified trap states on the QDs surface [41]. Thus, considering 8.52 ns to be excited state lifetime of the donor QDs, the estimated energy transfer rate is found to be 0.33 ns^{-1} , which is consistent with that from Tachiya model.

3.5. CD studies on the interaction between arginine capped QDs and DNA

In order to confirm any structural perturbation in the native structure of the dodecamer DNA adsorbed onto the QDs surface, we have performed circular dichroism (CD) studies. As revealed from Fig. 3a CD spectrum, the hybridized DNA used in our studies were in a B-form, evidenced by a negative band at 248 nm and a positive band at 280 nm [19,42], also the structural integrity of DNA B-form is almost retained in the QD–DNA nanobioconjugates. Fig. 3b shows the overall secondary structure of the QD conjugated dodecamer DNA at 20 °C and 70 °C temperatures. It is clear that

both the peaks at 252 nm and 280 nm are affected by the temperature-induced melting of the QD conjugated dodecamer DNA. The change in the molar ellipticity associated with the 252 nm peak has been monitored to construct the temperature-induced melting and rehybridization profiles of the QD conjugated dodecamer DNA, as shown in Fig. 3c (melting) and d (rehybridization). The melting of DNA is accompanied by structural changes involving unwinding of the helix, destruction of major and minor grooves, and finally the separation of the two strands resulting in the formation of two single strands of complementary sequence. The melting and rehybridization temperatures have been estimated to be 42.6 °C and 41.0 °C, respectively, for the QD conjugated dodecamer DNA and this is in good agreement with the dodecamer DNA alone reported previously [43]. Fig. 3c and d show that the dodecamer is rehybridized into its original form maintaining the same hysteresis as it follows during its melting, which indicates that the π stacking interaction between the complementary base pair of the two strands is greater than the electrostatic interaction of each strand with the QDs. Moreover, an electrostatic interaction between the positively charged groups of the Arg-capped QDs and the negatively charged DNA dodecamer, could have changed its conformation as well as its melting temperature and rehybridization pathway [44]. However, as revealed from the CD study, all of its characteristic conformational features remain the same, before and after conjugation with the QDs. So, it appears that hydrogen-bonding interactions (instead of electrostatic interactions) are playing the dominant role in the adsorption of DNA onto the surface of arginine-capped QDs involving the protonated carboxyl

surface groups of the thin solubilizing layer of amino acids around the QDs [45].

4. Conclusion

In conclusion, we report a convenient approach for preparing water-soluble, biocompatible QDs following a liquid–liquid interfacial ligand exchange method, where L-arginine acts as a capping ligand. The successful conjugation of arginine with the QDs has been confirmed by FTIR spectroscopy. We have employed picosecond-resolved spectroscopic measurements, to demonstrate a highly efficient FRET from arginine-capped CdSe/ZnS QDs (donor) to EB-DNA (acceptor). The corresponding donor–acceptor distance has been calculated to be 2.42 nm, which suggest an adsorptive interaction between the dodecamer DNA molecules and arginine-capped QDs. From CD spectroscopic studies it is found that the dodecamer DNA retained their structural integrity upon conjugation with the QDs. Moreover, temperature induced melting and rehybridization of the QD conjugated dodecamer DNA suggest that hydrogen-bonding interaction could be the associated mechanism operating during the formation of QD–DNA nanobioconjugates. Considering the spread in use of QDs and the number of applications employing QD bioconjugates, understanding the interactions between QDs and biomolecules is of considerable importance and multidisciplinary interest. So, it is expected that this study may prove to be useful in making sensitive FRET-based sensors.

Acknowledgements

AG thanks UGC, India, for fellowship. NG thanks CSIR, India, for fellowship. We thank DST for a financial grant (SR/SO/BB-15/2007), the NTH School “Contacts in Nanosystems”, and the DFG. We thank Professor M. Tachiya for help in developing a theoretical approach for the analysis of our experimental data.

References

- [1] H. Mattoussi, J.M. Mauro, E.R. Goldman, G.P. Anderson, V.C. Sundar, F.V. Mikulec, M.G. Bawendi, *J. Am. Chem. Soc.* 122 (2000) 12142–12150.
- [2] D.V. Talapin, A.L. Rogach, A. Kornowski, M. Haase, H. Weller, *Nano Lett.* 1 (2001) 207–211.
- [3] T. Jamieson, R. Bakhshi, D. Petrova, R. Pockock, M. Imani, A.M. Seifalian, *Biomaterials* 28 (2007) 4717–4732.
- [4] H. Li, Y. Yao, C. Han, J. Zhan, *Chem. Commun.* (2009) 4812–4814.
- [5] P. Brown, P.V. Kamat, *J. Am. Chem. Soc.* 130 (2008) 8890.
- [6] X. Michalet, et al. *Science* 307 (2005) 538–544.
- [7] Q. Shen, J. Kobayashi, L.J. Diguna, T. Toyoda, *J. Appl. Phys.* 103 (2008) 084304.
- [8] W.C.W. Chan, S.M. Nie, *Science* 281 (1998) 2016–2018.
- [9] G.P. Mitchell, C.A. Mirkin, R.L. Letsinger, *J. Am. Chem. Soc.* 121 (1999) 8122–8123.
- [10] D. Zhou, J.D. Piper, C. Abell, D. Klenerman, D.-J. Kang, L. Ying, *Chem. Commun.* (2005) 4807–4809.
- [11] I.L. Medintz, A.R. Clapp, H. Mattoussi, E.R. Goldman, B. Fisher, J.M. Mauro, *Nat. Mater.* 2 (2003) 630–638.
- [12] W.R. Algar, U.J. Krull, *ChemPhysChem* 8 (2007) 561–568.
- [13] H. Li, X. Wang, Z. Gao, Z. He, *Nanotechnology* 18 (2007) 205603 (6pp).
- [14] X.Y. Wu, H.J. Liu, J.Q. Liu, K.N. Haley, J.A. Treadway, J.P. Larson, N.F. Ge, F. Peale, M.P. Bruchez, *Nat. Biotechnol.* 21 (2003) 41–46.
- [15] W.W. Yu, E. Chang, J.C. Falkner, J. Zhang, A.M. Al-Somali, C.M. Sayes, J. Johns, R. Drezek, V.L. Colvin, *J. Am. Chem. Soc.* 129 (2007) 2871–2879.
- [16] X. Gao, Y. Cui, R.M. Levenson, L.W.K. Chung, S. Nie, *Nat. Biotechnol.* 22 (2004) 969–976.
- [17] B. Dubertret, P. Skourides, D.J. Norris, V. Noireaux, A.H. Brivanlou, A. Libchaber, *Science* 298 (2002) 1759–1762.
- [18] R. Mahtab, H.H. Harden, C.J. Murphy, *J. Am. Chem. Soc.* 122 (1999) 14–17.
- [19] S.S. Narayanan, S.S. Sinha, P.K. Verma, S.K. Pal, *Chem. Phys. Lett.* 463 (2008) 160–165.
- [20] H. Mattoussi, J.M. Mauro, E.R. Goldman, T.M. Green, G.P. Anderson, V.C. Sundar, M.G. Bawendi, *Phys. Status Solidi B* 224 (2001) 277–283.
- [21] J.a. Liu, H. Li, W. Wang, H. Xu, X. Yang, J. Liang, Z. He, *Small* 2 (2006) 999–1002.
- [22] B.O. Dabbousi, J. RodriguezViejo, F.V. Mikulec, J.R. Heine, H. Mattoussi, R. Ober, K.F. Jensen, M.G. Bawendi, *J. Phys. Chem. B* 101 (1997) 9463–9475.
- [23] C.J. Murphy, *Anal. Chem.* 74 (2002) 520A–526A.
- [24] C.B. Murray, D.J. Norris, M.G. Bawendi, *J. Am. Chem. Soc.* 115 (1993) 8706–8715.
- [25] W.W. Yu, Y.A. Wang, X. Peng, *Chem. Mater.* 15 (2003) 4300–4308.
- [26] W.W. Yu, E. Chang, R. Drezek, V.L. Colvin, *Biochem. Biophys. Commun.* 348 (2006) 781–786.
- [27] H. Brooks, B. Lebleu, E. Vivès, *Adv. Drug Deliv. Rev.* 57 (2005) 559–577.
- [28] J.R. Lakowicz, *Principles of Fluorescence Spectroscopy*, 3rd ed., Kluwer Academic/Plenum, New York, 1999.
- [29] C.N.R. Rao, K.P. Kalyanikutty, *Acc. Chem. Res.* 41 (2008) 489–499.
- [30] N. Varghese, C.N.R. Rao, *Mater. Res. Bull.* 46 (2011) 1500–1503.
- [31] B. Trzaskowski, L. Adamowicz, P.A. Deymier, *J. Biol. Inorg. Chem.* 13 (2008) 133–137.
- [32] X. Ai, Q. Xu, M. Jones, Q. Song, S.-y. Ding, R.J. Ellingson, M. Himmel, G. Rumbles, *Photochem. Photobiol. Sci.* 6 (2007) 1027–1033.
- [33] P. Schapotschnikow, B. Hommersom, T.J.H. Vlught, *J. Phys. Chem. C* 113 (2009) 12690–12698.
- [34] J.Y. Rempel, B.L. Trout, M.G. Bawendi, K.F. Jensen, *J. Phys. Chem. B* 110 (2006) 18007–18016.
- [35] J.K. Cooper, A.M. Franco, S. Gul, C. Corrado, J.Z. Zhang, *Langmuir* 27 (2011) 8486–8493.
- [36] C. Bullen, P. Mulvaney, *Langmuir* 22 (2006) 3007–3013.
- [37] S. Kumar, S.B. Rai, *Indian J. Pure Appl. Phys.* 48 (2010) 251–255.
- [38] D. Kalaiselvi, R.M. Kumar, R. Jayavel, *Cryst. Res. Technol.* 43 (2008) 851–856.
- [39] M. Tachiya, *Chem. Phys. Lett.* 33 (1975) 289–292.
- [40] M. Tachiya, *J. Chem. Phys.* 76 (1982) 340.
- [41] S. Sadhu, K.K. Haldar, A. Patra, *J. Phys. Chem. C* 114 (2010) 3891–3897.
- [42] R. Sarkar, S.K. Pal, *Biopolymers* 83 (2006) 675–686.
- [43] D. Banerjee, S.K. Pal, *J. Phys. Chem. B* 111 (2007) 10833–10838.
- [44] R. Prado-Gotor, E. Grueso, *Phys. Chem. Chem. Phys.* 13 (2011) 1479–1489.
- [45] W.R. Algar, U.J. Krull, *Langmuir* 22 (2006) 11346–11352.